Model-based Analysis for Real-time Label-free Ultraviolet Quantification of Ultrafast Plasmonic Polymerase Chain Reaction

P. Mohammadyousef[1], M. Paliouras[2], M. Trifiro[2], and A.G. Kirk[1]
[1]*Electrical and Computer Engineering Dept., McGill University, Montréal, Canada*
[2]*Lady Davis Inst. for Medical Research, Jewish General Hospital, Montréal, Canada*

***Abstract*— A mathematical model for DNA quantification was calibrated using experimental results from real-time 260nm absorption measurements of plasmonic PCR thermocycling. The effect of different PCR parameters on template amplification was investigated using the calibrated model.**

***Clinical Relevance*— The results will aid researchers to optimize PCR reagent concentrations and system conditions to achieve faster and more efficient amplification as well as more sensitive amplicon detection.**

I. Introduction

Real-time polymerase chain reaction, also known as quantitative PCR (qPCR), is used to determine relative quantification of enzymatically amplified double-stranded DNA (dsDNA) fragment carried out in three steps (denaturation, annealing, and elongation) controlled by temperature. In theory, considering the amplification efficiency of 100%, the target grows exponentially as the PCR cycles proceeds, i.e, the amount of PCR product after n cycles is 2^n times the initial DNA concentration [1, 2]. However, in practice limiting factors such as primer-dimer accumulation, non-uniform temperature regulation, exhaustion of reagents, thermal inactivation of the DNA polymerase decrease efficiency as the PCR cycles progress [3]. The PCR efficiency is instrument dependent and for an acceptable designed qPCR machine, the efficiency should fall above 90% [4]. Many stochastic and mathematical models have been presented to calculate expected efficiency to identify the factors reducing PCR yield. Most models reported an overall PCR performance in which the efficiency of the reaction remains constant throughout all PCR cycles [5-7]. These models are only applicable for the early cycles when the efficiency is nearly constant. Other models have considered the cycle dependency of PCR efficiency by incorporating the melting, annealing, and elongation steps efficiencies into overall efficiency [8, 9]. These models were used in qPCRs to analyze and detect parameters controlling or degrading denaturing, annealing, and extension efficiencies [10, 11]. In this study, we use a mathematical model presented by Booth et al. to investigate cycle to cycle efficiencies and PCR reagent concentrations of a real-time 260nm detection plasmonic PCR system [11, 12].

The plasmonic amplification is carried out by photothermal heating of evenly dispersed gold nanorods (AuNRs) in PCR reaction by an 808nm vertical-cavity surface emitting laser (VCSEL) irradiation [13-16]. The real time detection is based on measuring transmitted 260nm power from a UV LED through PCR solution by a photodetector [17, 18]. The UV transmittance exhibits a sigmoidal-shaped curve for successful PCRs and a monotonically increasing exponential curve for failed PCRs. The UV transmittance curve shapes and threshold cycles (C_t) serve as fingerprints to determine PCR results and the amount of amplified DNA, respectively. Model calibration based on captured UV transmittance data quantifies PCR parameters such as rates of primer and template annealing as well as polymerase binding. These parameters will help to optimize PCR ingredients' concentration for faster and more efficient PCR. Furthermore, the calibrated model was used to study the impact of template/polymerase plasmonic thermal/UV damage and annealing step duration on amplicon generation.

II. Materials and Methods

A. PCR Sample Preparation

The 20µL PCR mixture contained 1.6µL of HemoKlentaq polymerase (New England Biolabs, Ipswich, MA), 4µL of its buffer, 1.2µL of 5µM forward and reverse primers with sequences of 5'-TCCGGAGCGAGTTACGAAGA-3' and 5'-AATCAATGCCCGGGATTGGT-3', 0.5µL of 2mM dNTPs, and 4.5×10^5 copies of Chlamydia Trachomatis Strain LGV III (ATCC, Manassas, VA). Different DNA copy numbers are obtained by making 10-fold serial dilutions of 4.5×10^5 copy number stock solution. The plasmonic amplification of DNA is enabled by adding 1µL of 50nM Poly(enthylene glycol)-modified gold nanorods (PEG-AuNRs) purchased from Nanopartz (Loveland, CO) to obtain final concentration of 2.5nM of AuNRs. The ingredients were diluted with double distilled water to obtain the final volume of 20µL. The transverse and longitudinal surface plasmon absorption peaks of AuNRs are 507nm and 808nm. Final PCR reaction mixture is placed in a 0.2mL thin walled PCR tube. To avoid water evaporation the reaction was covered with 50µL of mineral oil.

B. Working principle

The photothermal amplification is performed by an 808nm 3W VCSEL and a fan. The plasmonic thermocycling is conducted by maintaining the denaturation, annealing, and elongation steps temperatures constant at 85°C±0.22, 60°C±0.11, and 72°C±0.24 for 1, 5, and 1s, respectively. Using only 2W of VCSEL's power, the average heating and cooling rates for 40 cycles are 6°C/s and 3.3°C/s, respectively. For real-time amplicon detection, 260nm LED irradiated the tube for 50ms to collect the UV transmittance readings of every cycle by a 150-550nm gain amplified photodetector. The

UV transmittance data is plotted against cycles to generate amplification curves (Fig. 1). The shape of curves reveals PCR results (successful or failed). 40 cycles of amplification and detection of 10^5 copies of *Chlamydia Trachomatis* DNA with an extension length of 300 base pair (bp) was achieved under 15mins.

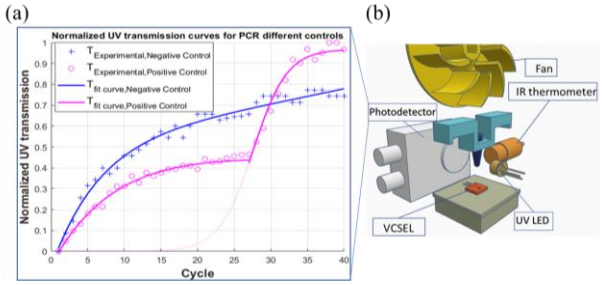

Figure 1. (a) UV transmittance data for positive (pink) and negative (blue) controls with least square fitted curves (solid line). (b) Design layout of VCSEL-based thermocycler and UV detection system.

III. MODEL CALIBRATION

The model reported by Booth et al. is valid with the following assumptions: i) DNA and polymerase damage are independent of PCR cycles ii) absence of primer-dimer events and primer-template annealing during elongation step iii) constant extension rate iv) irreversible annealing and elongation reactions v) the concentration of forward and reverse primers are equal, and they bind to equal number of complementary single-stranded DNA (ssDNA) molecules, and finally vi) during melting step, all dsDNA molecules are converted to ssDNA. Model parameters are classified into experimental (known) and predicted (unknown) groups. Table I demonstrates the experimental variables set in the real-time UV monitoring plasmonic PCR device. The five unknown parameters are shown in Table II. To simplify the calibration process, the polymerase binding rates at annealing and elongation temperatures (60 and 72°C) are considered equal (K_C=K_C^*). In Table I and Table II, we used the same nomenclature as Booth et al. [11, 12].

TABLE I. PLASMONIC UV SYSTEM KNOWN PARAMETERS

Experimental Parameters	*Description*	*Value*	*Unit*
S_0	Initial DNA concentration/Copy number	8.3e-9/ 10^5	µM
P_0	Starting Primer Concentration	0.15	µM
E_0	Initial polymerase concentration	0.5	µM
V	Polymerase extension rate	500	bp/s
l_{DNA}	Template length	221	bp
l_{primer}	Primer length	20	bp
t_a,t_e	Annealing/Elongation duration	5/1	s

TABLE II. UNKNOWN PARAMETERS

Predicted Parameters	*Description*	*Unit*
K_p	Primer annealing rate	µM/s
K_S	ssDNA annealing rate	µM/s
K_C and K_C^*	Polymerase annealing rate at annealing and elongation steps	µM/s
η_d	ssDNA thermal damage	-
η_{dE}	Polymerase thermal damage	-

Different experiments with varying initial DNA concentrations were undergone plasmonic amplification, and the amplification curves (transmittance vs. cycles, $T_{Experimental}$) were obtained experimentally (Table III). The same experiments were used to calibrate the unknown parameters.

TABLE III. EXPERIMENTS FOR QUANTIFYING UNKNOWN PARAMETERS

Experiments No.	*Different DNA starting copy number*
1	10^5
2	10^4
3	10^3
4	10^2
5	10
6	1

For each set of predicted unknown parameters, the model calculates DNA concentration per PCR cycle, and from DNA concentration, the concentration of consumed free nucleotides is calculated using primer and template length difference.

$$[dNTPs]=S\times(l_{DNA}-l_{primer}) \quad (1)$$

It is known that the PCR reagents with highest 260nm absorption are nucleotides and Taq polymerase due to their heterocyclic rings and aromatic amino acid network, respectively [19-21]. Therefore, in order to calculate the 260nm transmittance of the model for the calculated dNTPs and Taq concentrations, the absorbance (A) of varying dNTPs and Taq concentrations were measured using UV spectrophotometer (DS-11 Series, DeNovix Inc.). Equation (2) and (3) show linear relation between A_{dNTPs} and A_{Taq} and their corresponding concentrations.

$$A_{dNTPs}=3.69[dNTPs]_{mM}+0.125 \quad (2)$$

$$A_{Taq}=1.21[Taq]_{\mu M}+2.34 \quad (3)$$

Using the superposition of dNTPs and Taq absorbance with respect to optical path length of UV system and the spectrometer ($OPL_{UV\ sys.}$ and $OPL_{Spectrometer}$), transmittance of the model (T_{Model}) is calculated as follows:

$$A_{total}=A_{dNTPs}+A_{Taq} \quad (4)$$

$$A_{UV\ system}=\frac{OPL_{UV\ system}}{OPL_{Spectrometer}}\times A_{total} \quad (5)$$

$$T_{Model}=10^{-A_{UV\ system}} \quad (6)$$

The calculated transmittance (T_{Model}) is normalized and plotted against cycles. The set of unknown parameters demonstrating the least square error fit between T_{Model} and $T_{Experimental}$ are presented in Table IV. Fig. 2 illustrates $T_{Experimental}$ (solid line) and T_{Model} (plus signs) with the defined unknown parameters in Table IV for different initial DNA concentrations.

TABLE IV. DETERMINED UNKNOWN PARAMETERS BY LEAST SQUARE FITTING T_{MODEL} TO $T_{EXPERIMENTAL}$

Calculated Parameters	*Value*	*Unit*
K_p	4.21±0.87	µM/s
K_S	4.18±0.86	µM/s
$K_C=K_C^*$	10.34	µM/s
η_d	1	-
η_{dE}	0.95	-

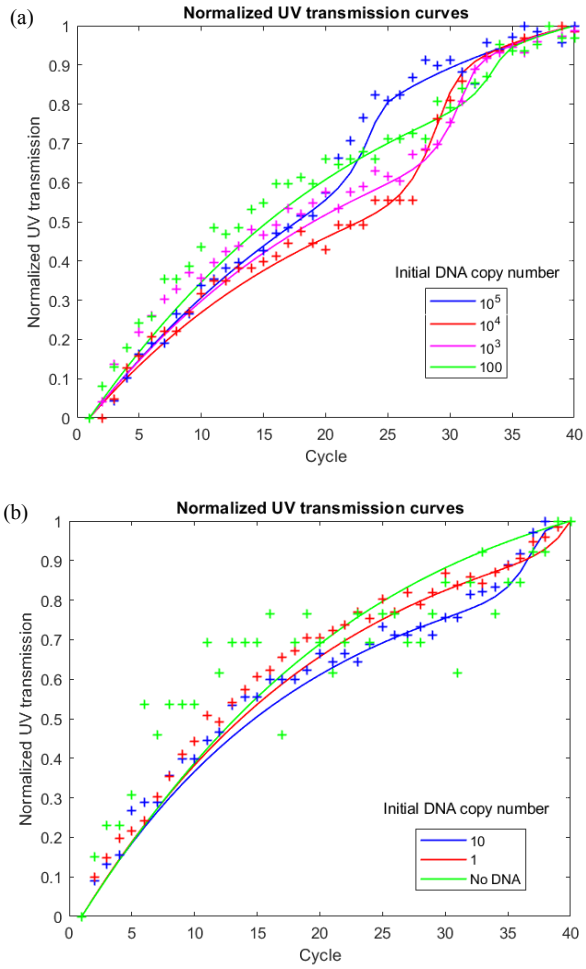

Figure 2. Comparison of T_{Model} and $T_{Experimental}$ for (a) 10^5 to 100 and (b) 10 to zero initial DNA copy number.

IV. RESULTS

Once the model is calibrated, the limiting factors controlling the PCR yield can be analyzed. In this section, the initial DNA copy number is set at 10^4, and the rest of the model parameters are equal to Table I and IV. Since the source of heat generation is non-radiative decay of localized surface plasmons, the localized hot spots in close proximity of DNA result in DNA thermal damage. Based on Booth et al. model the denaturing efficiency (η_d) is DNA thermal damage, and Fig. 3 shows with smaller η_d, the threshold cycle (C_t) is constant; however, after C_t fewer dsDNAs are formed.

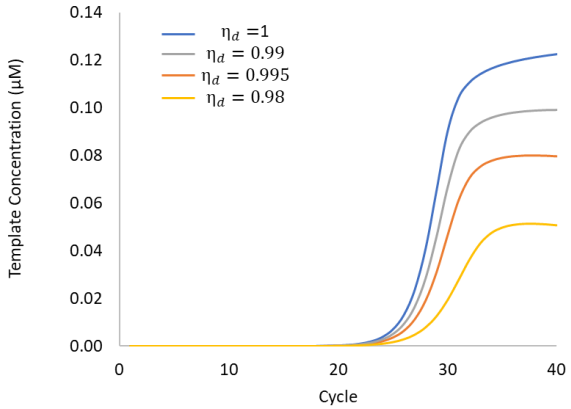

Figure 3. Relation between DNA thermal damage and amplicon generation.

Like DNA, polymerase is vulnerable to thermal damage in plasmonic amplification. Fig. 4 demonstrates for polymerase denaturing damage of less than 0.89, the DNA replication ceases and starts to decrease after cycle 30 due to thermal inactivation of the DNA polymerase.

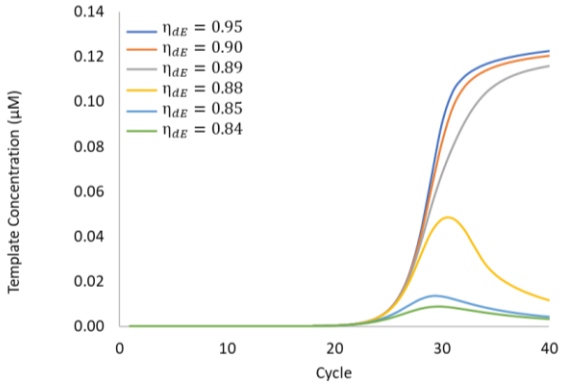

Figure 4. Template concentration vs. polymerase denaturing damage.

The other parameter which impacts the elongation efficiency is UV damage to DNA helix which induces formation of pyrimidine dimers [19, 20]. Therefore, we introduced a new UV damage factor (η_{dUV}) into the model. As a result, elongation efficiency at cycle j (η_e^j) is defined as the product of UV damage factor and completely extended ternary complex molecules (C_C^j) divided by the total ternary complex molecules formed at the end of elongation step (C_e^j).

$$\eta_e^j=\eta_{dUV}\frac{C_C^j}{C_e^j} \quad (7)$$

The UV damage to ternary complexes not only reduces number of generated dsDNAs but also right shifts the C_t value (Fig. 5). Thus, samples with identical initial DNA concentration, PCR protocol, and reagents, but dissimilar UV exposure time show different C_t values, and this reduces the sensitivity in amplicon quantification.

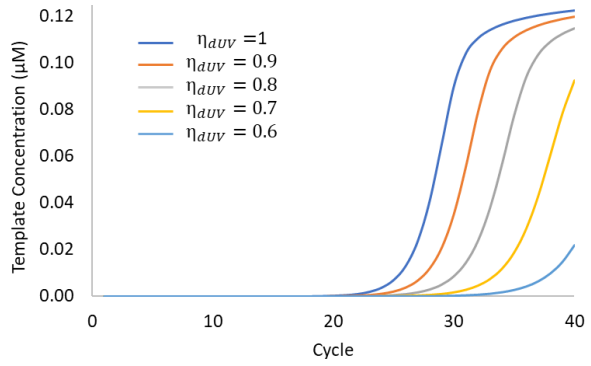

Figure 5. UV damage factor changes PCR efficiency and C_t.

One advantage of amplifying dsDNA plasmonically is the short amplification time. In our photonic qPCR procedure, the duration of annealing step (t_a) is 5 times more than the other two PCR steps. Therefore, t_a as the most time-consuming step duration is worth of study to understand how it governs dsDNA generation. The results in Fig. 6 indicates that both amplified template concentration and threshold cycle are affected by the amount of time dedicated to primer-template annealing. For time duration less than 3s, the amplification profile never reaches plateau phase under our plasmonic UV detection system's condition.

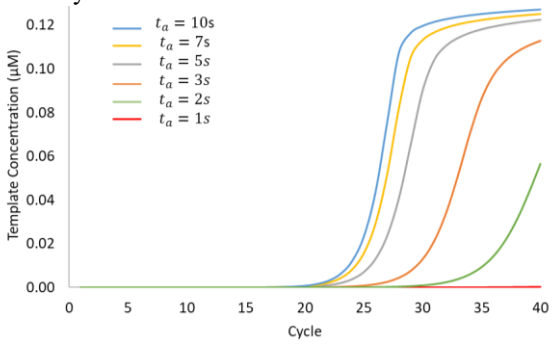

Figure 6. Amplification profiles for different t_a.

V. Conclusion

The use of mathematical model uncovers how PCR conditions impact PCR efficiency and detection sensitivity in our plasmonic qPCR such as thermal and UV damage to DNA due to plasmonic amplification and UV detection. Therefore, these model analyses will help to change PCR protocols to maximize DNA replication. In future publication, the presented results will be experimentally validated. Also, UV amplification curves for other PCR conditions such as different types of DNA and polymerases along with varying template lengths will be experimented and compared with model generated UV curves.

Acknowledgment

This study is supported by Génome Québec and Génome Canada (DIG-Phase 1- 9516).

References

[1] Q. Phenix-Lan, S. Martin, and B. Eric, "dPCR: A Technology Review," *Sensors*, vol. 18, no. 4. doi: 10.3390/s18041271

[2] P. Boisseau, P. Houdy, M. Lahmani, and S. European Materials Research, Nanoscience : nanobiotechnology and nanobiology, Berlin ;: Springer, 2009. [Online]. Available.

[3] J. Linda and H. Johannes, "Challenging the proposed causes of the PCR plateau phase," *Biomolecular Detection and Quantification*, vol. 17. doi: 10.1016/j.bdq.2019.100082

[4] D. Svec, A. Tichopad, V. Novosadova, M. W. Pfaffl, and M. Kubista, "How good is a PCR efficiency estimate: Recommendations for precise and robust qPCR efficiency assessments," *Biomolecular detection and quantification,* vol. 3, pp. 9-16, 2015.

[5] G. Stolovitzky and G. Cecchi, "Efficiency of DNA Replication in the Polymerase Chain Reaction," *Proceedings of the National Academy of Sciences of the United States of America,* vol. 93, no. 23, pp. 12947-12952, 1996.

[6] P. Jagers and F. Klebaner, "Random variation and concentration effects in PCR," *Journal of Theoretical Biology,* vol. 224, no. 3, pp. 299-304, 2003.

[7] M. W. Pfaffl, "A new mathematical model for relative quantification in real-time RT-PCR," *Nucleic acids research,* vol. 29, no. 9, p. e45, 2001.

[8] W. Liu and D. A. Saint, "Validation of a quantitative method for real time PCR kinetics," *Biochemical and Biophysical Research Communications,* vol. 294, no. 2, pp. 347-353, 2002.

[9] A. E. Platts, G. D. Johnson, A. K. Linnemann, and S. A. Krawetz, "Real-time PCR quantification using a variable reaction efficiency model," *Analytical biochemistry,* vol. 380, no. 2, pp. 315-22, 2008.

[10] A. Hassibi, H. Kakavand, and T. Lee, "A stochastic model and simulation algorithm for polymerase chain reaction (PCR) systems," *Proc. of IEEE Workshop on Genomics Signal Processing and Statistics,* 01/01 2004.

[11] T. M. Louw, C. S. Booth, E. Pienaar, J. R. TerMaat, S. E. Whitney, and H. J. Viljoen, "Experimental validation of a fundamental model for PCR efficiency," *Chemical Engineering Science,* vol. 66, no. 8, pp. 1783-1789, 2011.

[12] C. S. Booth, E. Pienaar, J. R. Termaat, S. E. Whitney, T. M. Louw, and H. J. Viljoen, "Efficiency of the polymerase chain reaction," *Chemical Engineering Science,* vol. 65, no. 17, pp. 4996-5006, 2010.

[13] P. Mohammadyousef, G. Uchehara, M. Paliouras, M. Trifiro, and A. Kirk, *Ultrafast VCSEL-based plasmonic polymerase chain reaction with real-time label-free amplicon detection for point-of-care diagnostics* (SPIE BiOS). SPIE, 2020.

[14] P. J. Roche *et al.*, "Demonstration of a plasmonic thermocycler for the amplification of human androgen receptor DNA," *The Analyst,* vol. 137, no. 19, pp. 4475-81, 2012.

[15] P. J. R. Roche *et al.*, "Real time plasmonic qPCR: how fast is ultra-fast? 30 cycles in 54 seconds," *The Analyst,* vol. 142, no. 10, pp. 1746-1755, 2017.

[16] G. Uchehara, A. Kirk, M. Trifiro, M. Paliouras, and P. Mohammadyousef, *Real time label-free monitoring of plasmonic polymerase chain reaction products* (SPIE Smart Structures + Nondestructive Evaluation). SPIE, 2019.

[17] M. Tran, M. Paliouras, P. Mohammadyousef, M. Trifiro, and A. G. Kirk, "Real-time fluorophore-free optical monitoring of ultrafast DNA amplification for qPCR," presented at the 2nd European Biosensor Symposium 2019, EBS2019, Florence, Italy, 2019.

[18] P. Mohammadyousef, M. Paliouras, M. Trifiro, and A. Kirk, *Ultrafast plasmonic and real-time label-free polymerase chain reaction* (SPIE BiOS). SPIE, 2020.

[19] B. C. M. Pang and B. K. K. Cheung, "One-step generation of degraded DNA by UV irradiation," *Analytical Biochemistry,* Article vol. 360, no. 1, pp. 163-165, 2007.

[20] L. C. Burgess and J. O. Hall, "UV light irradiation of plastic reaction tubes inhibits PCR," *BioTechniques,* Article vol. 27, no. 2, pp. 252-256, 1999.